RESEARCH ARTICLE

Highly Transparent Sm:LuAG Ceramics for Cladding Fabricated by Solid-state Reactive Sintering

Junhao Ye[1,2], Weiwei Han[2,3], Zhenzhen Zhou[1,2], Chen Hu[1,2], Yiyang Liu[1], Lexiang Wu[1], Dong Huang[1], Tingsong Li[1] and Jiang Li[1,2,*]

[1] State Key Laboratory of High Performance Ceramics, Shanghai Institute of Ceramics, Chinese Academy of Sciences, Shanghai 201899, China
[2] Center of Materials Science and Optoelectronics Engineering, University of Chinese Academy of Sciences, Beijing 100049, China
[3] School of Microelectronics, Shanghai University, Shanghai 201800, China

Abstract

In solid-state laser systems with nanosecond repetition rates and high energy, amplified spontaneous emission (ASE) and parasitic oscillation (PO) produced by the gain material can significantly impact the laser output. A well-designed cladding composite structure is an effective solution to absorb ASE and suppress PO. In this work, 5 at.% Sm:LuAG transparent ceramics, a promising cladding material for suppressors of PO at 1064 nm of Nd:LuAG lasers, have been prepared by solid-state reactive sintering at 1825 °C followed by hot isostatic pressing (HIP) post-treatment at 1750 °C. The influences of TEOS (tetraethyl orthosilicate) content on microstructure evolution, in-line transmittance of the 5 at.% Sm:LuAG ceramics were studied. The results show that when the TEOS content is 0.8 wt.%, high transparency Sm:LuAG ceramics can be obtained by vacuum sintering at 1825 °C for 5 h followed by HIP post-treatment at 1750 °C in an argon atmosphere under 200 MPa for 3 h. The optimum in-line transmittance of the HIP-ed Sm:LuAG ceramics (1.5 mm thickness) is 83.3% at a wavelength of 808 nm and absorption coefficient of 3.46 cm^{-1} at 1064 nm, indicating that it can effectively suppress ASE and PO.

Keywords: Sm:LuAG, transparent ceramics, cladding ceramics, microstructure evolution, sintering additives.

1 Introduction

Since the first ruby laser device was invented in 1960, solid-state lasers (SSLs) have developed rapidly [1–3]. At present, SSLs with high peak power, high average power and high repetition rate are required to suit the requirements of material processing, lidar, and medical treatment. Laser gain materials for high average power and high repetition rate laser output, mainly containing garnet (YAG and LuAG) [4–6], fluoride (CaF_2) [7, 8], sesquioxide (Lu_2O_3, Y_2O_3 and Sc_2O_3) [9–12], are crucial for

Submitted: 29 October 2025
Accepted: 08 December 2025
Published: 20 December 2025

Vol. 1, **No.** 1, 2025.
10.62762/JAMR.2025.567536

***Corresponding author:**
✉ Jiang Li
lijiang@mail.sic.ac.cn

Citation
Ye, J., Han, W., Zhou, Z., Hu, C., Liu, Y., Wu, L., Huang, D., Li, T., & Li, J. (2025). Highly Transparent Sm:LuAG Ceramics for Cladding Fabricated by Solid-state Reactive Sintering. *Journal of Advanced Materials Research*, 1(1), 6–17.

energy conversion and laser generation, determining the laser output power, slope efficiency, and beam quality. To gain high average power and high repetition rate laser output, laser gain materials require appropriate saturation fluence, high optical quality and high thermal conductivity. Appropriate saturation fluence is a very important parameter for high repetition-rate nanosecond high-energy SSLs, because high saturation fluence limits the light extraction efficiency, while low saturation fluence decreases the light amplification efficiency, complicates the laser system, and increases light loss. For laser systems operating at room temperature, one of the most used gain materials is Nd:YAG, but its relatively low saturation fluence limits its scaling performance to high energy laser applications [13–15]. Nd:LuAG has recently been demonstrated with appropriate scaling performance, as its saturation fluence of 1.93 J/cm^2 is three times that of Nd:YAG [16]. It has been proved Nd:LuAG has smaller splitting of $^4F_{3/2}$ state (67 cm^{-1}) than that of Nd:YAG (84 cm^{-1}) [17], which produces a higher amplification at 1064 nm lasing wavelength. In conclusion, Nd:LuAG ceramics has shown great potential as the gain medium in high energy amplifier with strong capacity of energy storage, due to its moderate emission cross section (9.67×10^{-20} cm^2) [18–20]. Nd:LuAG transparent ceramics have been confirmed by Tsinghua University to be a promising gain material for high-energy, high-repetition-rate nanosecond SSLs, which has successfully achieved a maximum energy output of 10.3 J and a pulse width of 10 ns at room temperature [13, 14].

In high-power, high-repetition-rate solid-state laser systems, the thermal effect imposes a limit on the power density dissipated within the gain element [21–24]. However, this limitation can be reduced by increasing the size of the gain medium, which also enhances heat dissipation [25–27]. On the other hand, when the aspect ratio of the gain medium is large, spontaneous fluorescence can be amplified to very high power. The spontaneous fluorescence propagating transversely to the main beam leads to amplified spontaneous emission (ASE) and parasitic oscillation (PO), which depletes the upper laser level population [28, 29]. To mitigate this problem, cladding on the lateral surface of the gain medium is one of the strategies to suppress lateral reflection and improve laser performance, which has been proven to be effective by many research institutions [30–32]. Based on the design requirements, the cladding layers should meet the following criteria: (1) high absorption coefficient at the laser emission wavelength, (2) approximate refractive index that matches the gain medium, (3) seamless integration with the gain medium to minimize optical losses, and (4) high transparency at pump wavelength especially for the edge-pumped mode [33, 34].

The absorption spectra of YAG transparent ceramics doped with various metal ions (Sm^{3+}, Co^{2+}, Co^{3+}, Cr^{3+}, and Cr^{4+}) were investigated by Yagi et al. [25] in 2006. According to the research, Sm:YAG transparent ceramics were selected as the promising cladding material for Nd:YAG laser ceramics due to the highest absorption coefficient (3.6 cm^{-1}) at 1064 nm. A high laser output power of 67 kW was achieved by using the Sm:YAG-Nd:YAG composite ceramics with a volume of 120 × 120 × 20 mm^3 [35]. Because Nd-doped LuAG/YAG ceramics exhibit similar emission spectra, and Sm-doped LuAG/YAG also shows comparable absorption spectra, Sm:LuAG is regarded as an ideal cladding material for Nd:LuAG. In 2013, Gonçalvès-Novo et al. [36] using Yb:YAG AM Lucia laser amplifier achieved 14 J at 2 Hz laser output. Ma et al. [37] reported in 2017 a 10.3 mJ amplified pulse using the Nd:LuAG ceramic seeded by a 5.2 mJ Nd:YAG Q-switched oscillator, corresponding to a pulse peak power of 1.47 MW. In 2019, a 10.3 J, 10 Hz output was achieved using the Nd:LuAG ceramic nanosecond laser amplifier [13]. Kong et al. [38] also utilized Sm:YAG cladding ceramics to suppress ASE of parasitic ring modes at 1064 nm, achieving a single-pulse energy of 1.66 mJ with a repetition rate of 10 Hz.

For low reflection at the boundary, the refractive index of the cladding material must match that of the gain material, which means the host material for cladding should be the same as the gain material. Compared to single crystals, it is easier and cheaper to produce large-sized ceramics while having the same good performance as single crystals [25, 39]. Thus, transparent ceramics are promising laser gain material for high-power lasers systems. According to the research mentioned above, Sm:LuAG ceramics exhibit superior characteristics like a high absorption coefficient at 1064 nm and high transparency at the pump wavelength of 808 nm, making Sm:LuAG ceramics very effective in suppressing the ASE and PO effect.

The synthesis of transparent Sm:LuAG ceramics typically involves the use of sintering additives such

as CaO and TEOS (tetraethyl orthosilicate) to achieve high transparency at pump wavelength. Compared to SiO_2 powders, liquid TEOS is easier to mix uniformly with other raw material powders during the ball-milling. The more uniform distribution of Si^{4+} promotes uniform grain growth and enables effective pores removal. Consequently, liquid TEOS helps avoid problems such as the formation of intragranular pores, which typically arise from different rates of grain growth in ceramics. Therefore, in this study, TEOS has been chosen to be the sintering aid instead of SiO_2 powders. While the influence of sintering aids on the YAG and LuAG ceramic sintering process has been widely investigated [40–42]. However, the effect of TEOS on the kinetics and microstructural evolution of Sm:LuAG ceramics during sintering has not been explored. In this study, the 5 at.% Sm:LuAG transparent ceramics were fabricated with commercial Lu_2O_3, α-Al_2O_3 and Sm_2O_3 powders using TEOS and CaO as sintering additives. The influences of TEOS content on microstructure evolution, in-line transmittance and absorption spectra of the 5 at.% Sm:LuAG ceramics were systematically investigated [43].

2 Experimental

High-purity commercial Lu_2O_3 (99.999%, Sheeny Metal Material Co., Ltd., Shanghai, China), α-Al_2O_3 (99.99%, Sumitomo Chemical Co., Ltd., Tokyo, Japan) and Sm_2O_3 (99.99%, Sheeny Metal Material Co., Ltd., Shanghai, China) powders were used as raw powders in this work. 0.4-1.0 wt.% TEOS (99.99%, Alfa Aesar) and CaO (99.99%, Alfa Aesar) were added as sintering additives. All the ceramic samples contain the same amount of CaO addition. The raw powders mixed with TEOS and CaO were ball-milled in ethanol for 12 h with a speed of 130 r/min using 5 mm diameter alumina balls as the milling medium. The weight ratio of alumina balls and powders was 3:1. After ball-milling the raw powder and sintering additives, the slurry was dried at 80 °C and sieved through 200-mesh screen to obtain homogeneous powders. The powders were then calcined at 600 °C for 4 h in air, followed by dry pressing into disks with the diameter of 18 mm under 40 MPa and further cold isostatic pressing under 250 MPa. The green compacts were pre-sintered under vacuum at 1825 °C for 5 h to acquire transparent ceramics and then hot isostatic pressing (HIP) post-treated at 1750 °C in an argon atmosphere of 200 MPa for 3 h to eliminate residual pores and improve the optical quality of Sm:LuAG transparent ceramics. Finally, the Sm:LuAG transparent ceramics were air annealed at 1400 °C for 10 h to eliminate oxygen vacancies and then were mirror-polished into 1.5 mm for further characterization.

The morphology of the starting powders and microstructures of polished ceramics were observed by a field emission scanning electron microscopy (FESEM, SU8220, Hitachi, Japan) equipped with an energy dispersive X-ray spectroscope (EDS, X-MaxN 80, Oxford Instruments, Britain). The phase composition of the sintered ceramics was identified by the X-ray diffraction (Cu Kα1 radiation (λ = 0.15405 nm), XRD, Bruker D8 Focus, Germany) in the range of 2θ = 10–80 using nickel-filtered Cu-Kα radiation. Before the FESEM observation, the ceramics were thermally etched at 1400 °C for 10 h in air. The average grain sizes were measured by the common linear intercept analysis (more than 200 grains were counted) according to the equation GS = 1.56 L, where L is the mean intercept. The in-line transmittance and absorption curves of the mirror-polished samples were measured by a UV-VIS-NIR spectrophotometer (Model Cary-5000, Varian, USA). The optical scattering sources of polished ceramics were observed by a transparent microscope (Optical Microscope, BX51TF, Olympus, Japan).

3 Results and discussion

Figure 1 shows the FESEM micrographs of the raw powders of Sm_2O_3, Lu_2O_3 and α-Al_2O_3 and the powder mixture after ball milling. The particle size of the α-Al_2O_3 raw powders is uniformly distributed, while the average grain size is about 300 nm. As shown in Figures 1(b) and (c), both Lu_2O_3 and Sm_2O_3 powders are essentially agglomerated into irregular secondary particles with the particle sizes of several microns. As shown in Figure 1(d), the ball-milled powder is obviously smaller than the initial powders of Lu_2O_3 and Sm_2O_3, which proves the effect of ball milling on the crushing and mixing of raw material powders.

After obtaining the mixture of raw powders and different amounts of TEOS sintering additive, the powders were dry pressed and further cold isostatic pressed to obtain green compacts. The green compacts were then pre-sintered at the temperature of 1825°C for 5 h in vacuum to form garnet crystal structure and eliminate pores. The morphologies of vacuum-sintered 5 at.% Sm:LuAG ceramics, as shown in Figure 2, are characterized by a homogenous microstructure with minimal pores. No abnormal grain growth is observed from any of the ceramic

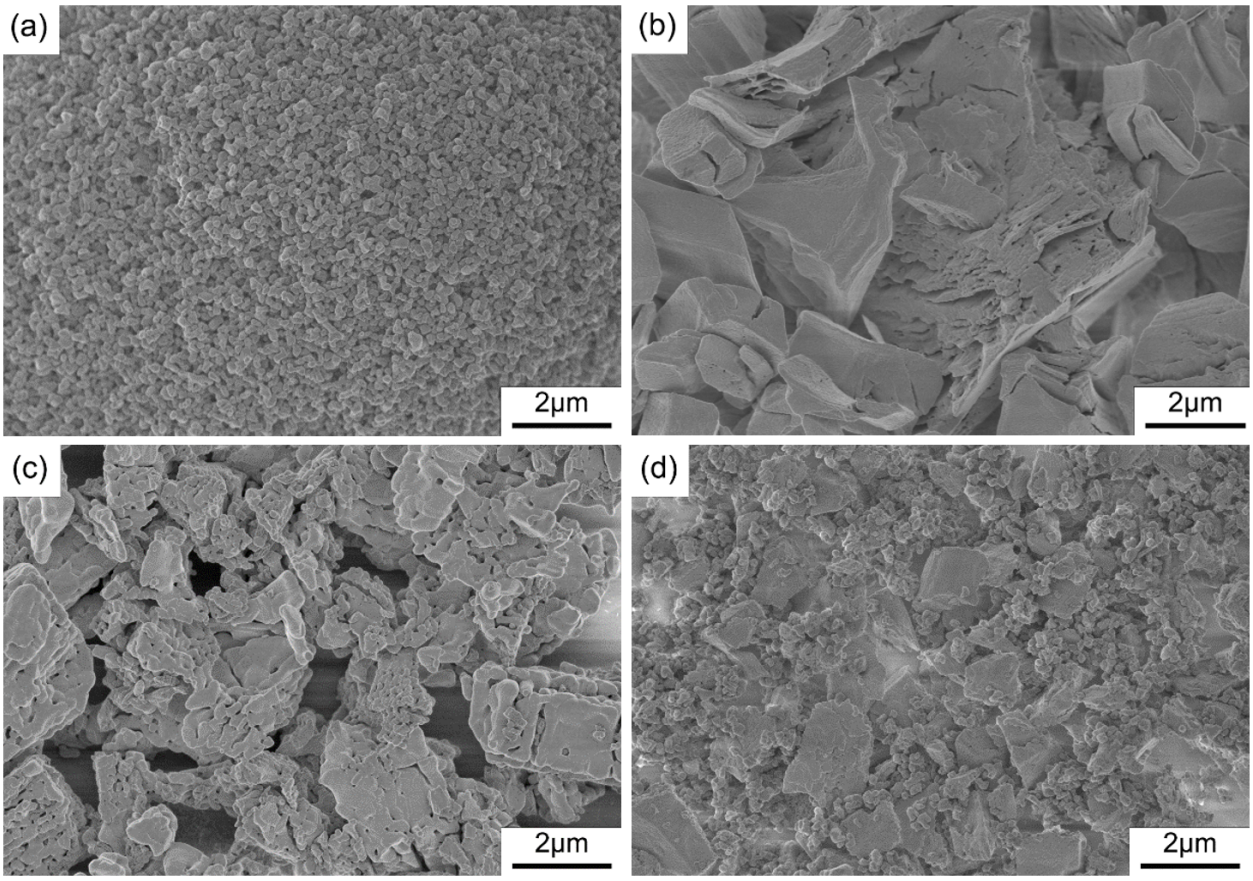

Figure 1. FESEM micrographs of the commercial powders (a) α-Al_2O_3, (b) Lu_2O_3, (c) Sm_2O_3 and (d) powders mixture after ball milling.

samples. Furthermore, in Sm:LuAG ceramics doped with 0.4–1.0 wt.% TEOS, no secondary phases were detected along grain boundaries or in triple grain boundaries. From the FESEM micrographs of pre-sintering ceramics, all ceramics have a relatively dense microstructure, but there are still some intergranular pores between grain boundaries that have not been eliminated [44]. Therefore, HIP post-treatment for the vacuum pre-sintering ceramics is essential to obtain transparent ceramics with higher optical quality.

Figure 3 exhibits the XRD patterns of the 5 at.% Sm:LuAG ceramics with 0.4–1.0 wt.% TEOS pre-sintered at 1825 °C for 5 h and HIP post-treated at 1750 °C for 3 h. The diffraction peaks of the ceramics match well with the cubic LuAG standard card (PDF# 73-1368). No additional phases were revealed within the detection limit of XRD. All samples exhibit sharp diffraction peaks, indicating an excellent crystallinity after sintering.

The lattice constant of the ceramics was calculated based on the XRD patterns of the Sm:LuAG ceramics. Figure 4 shows the lattice constant of Sm:LuAG ceramics as a function of TEOS addition. The lattice parameters of all the Sm:LuAG ceramics are higher than that of undoped LuAG (11.9064 Å). This is because the ionic radius of Sm^{3+} at coordination number of 8 (0.96 Å) is larger than that of Lu^{3+} (0.85 Å). Consequently, when Lu^{3+} ions are replaced by Sm^{3+} ions in the LuAG lattice, the lattice expands and the lattice constants increase. With the TEOS content increasing from 0.4 to 1.0 wt.%, the lattice constants decrease accordingly from 11.9269 Å to 11.9199 Å. This is because the use of the SiO_2 sintering additive leads to the substitution of Al^{3+} (0.53 Å) ions by smaller Si^{4+} ions (0.4 Å) in the garnet structure, resulting in a decrease of the lattice parameter of the ceramics.

As shown in Figure 2, there are still some intergranular pores between grain boundaries after vacuum pre-sintering. High porosity will cause severe optical scattering and lead to unnecessary heat generation during laser working. Therefore, HIP post-treatment is necessary for further densification and can facilitate the reduction of the intergranular pores in the ceramics. Figure 5 shows the FESEM micrographs of the 5 at.% Sm:LuAG ceramics pre-sintered at 1825 °C for 5 h and HIP post-treated at 1750 °C for 3 h added

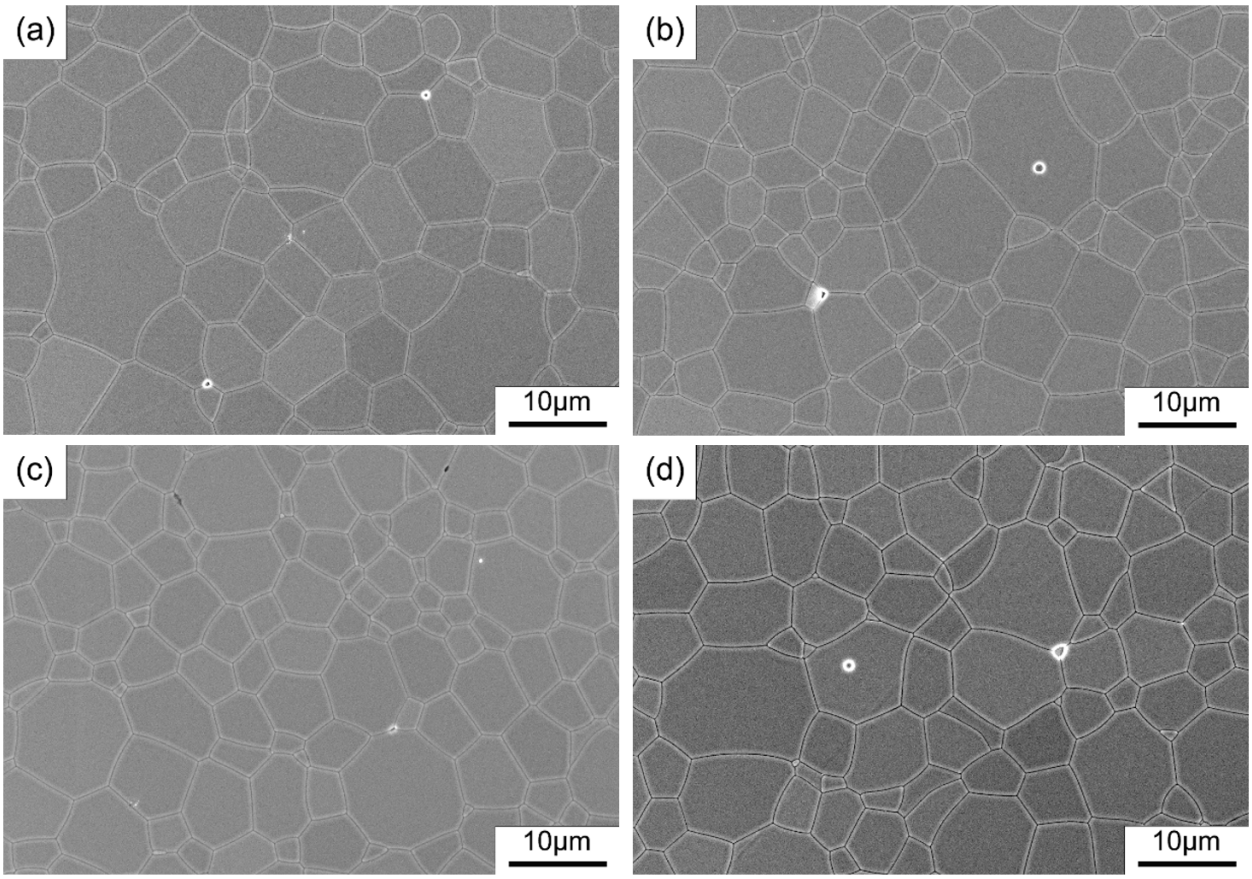

Figure 2. FESEM micrographs of the 5 at.% Sm:LuAG ceramics pre-sintered at 1825 °C for 5 h with the addition of (a) 0.4 wt.%, (b) 0.6 wt.%, (c) 0.8 wt.%, (d) 1.0 wt % TEOS.

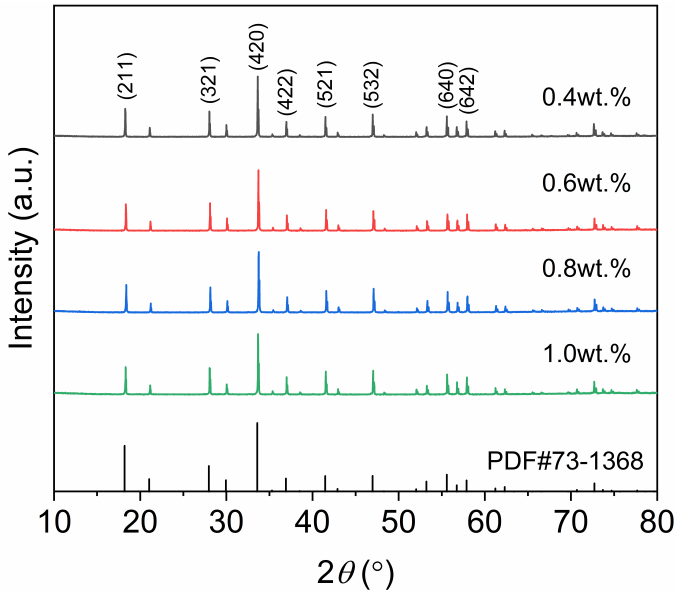

Figure 3. XRD patterns of the 5 at.% Sm:LuAG ceramics with 0.4–1.0 wt.% TEOS.

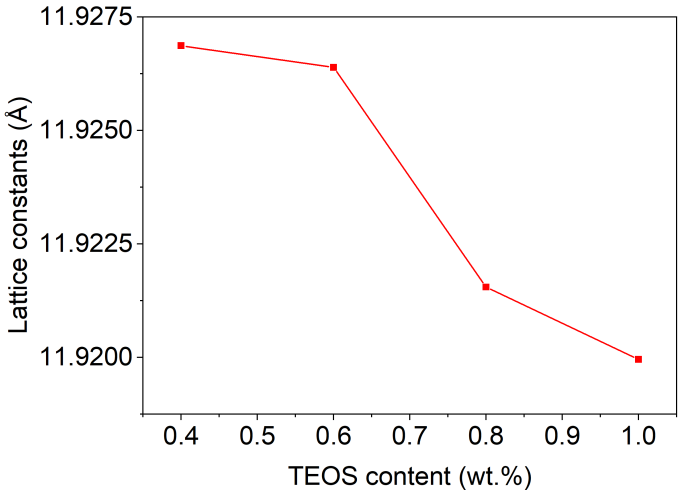

Figure 4. Lattice constants of the 5 at.% Sm:LuAG ceramics with 0.4–1.0 wt.% TEOS.

with 0.4–1.0 wt.% TEOS and 0.05 wt.% CaO. The Sm:LuAG ceramics with 0.6 and 0.8 wt.% TEOS exhibit dense microstructure, and no secondary phases at grain boundaries are found in those ceramics after HIP treatment. On the other hand, there are still some micropores after HIP for the ceramics with 0.4 and 1.0 wt. % TEOS. In addition, all the Sm:LuAG ceramics display a uniform microstructure and there is no exaggerated grain growth.

To better investigate the microstructure evolution in Sm:LuAG ceramics during sintering, the average grain

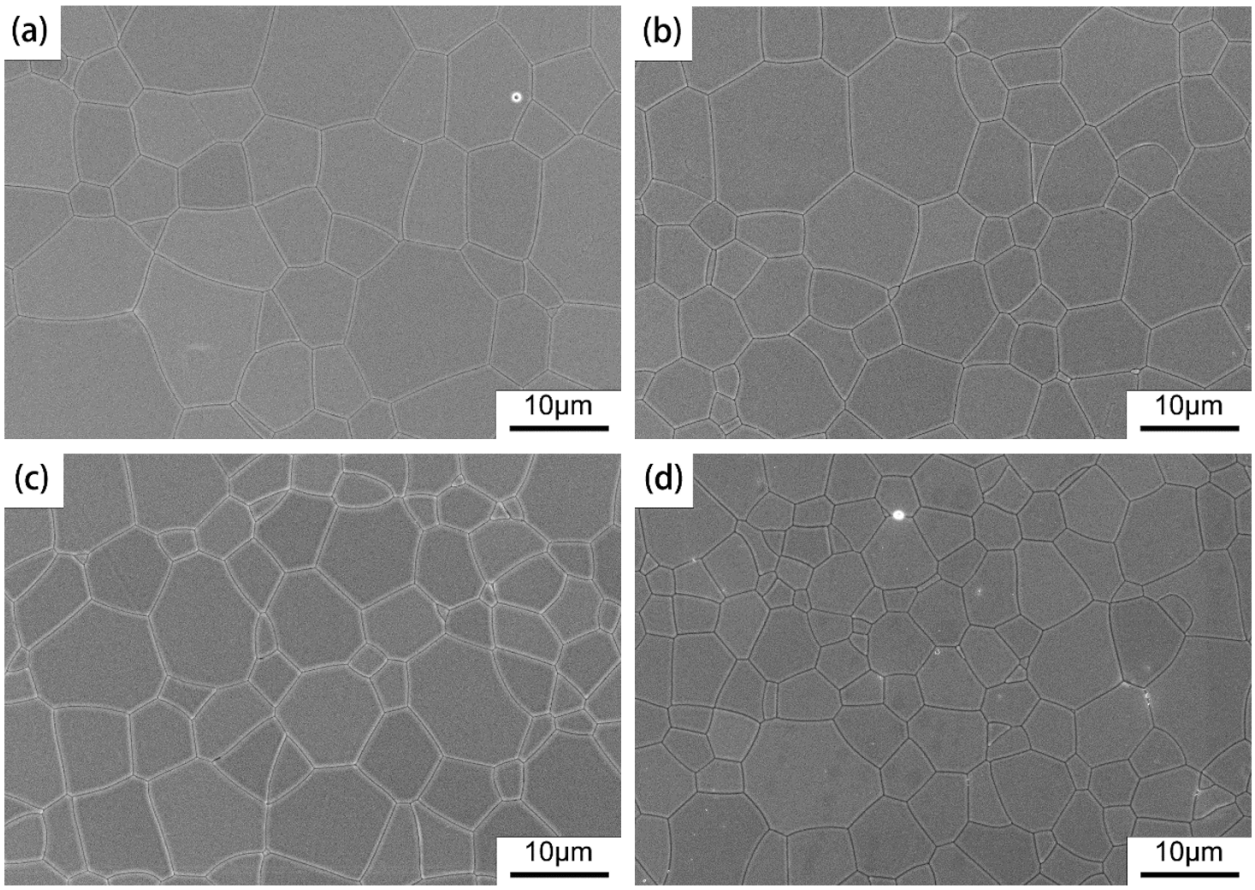

Figure 5. FESEM micrographs of the 5 at.% Sm:LuAG ceramics pre-sintered at 1825 °C for 5 h and HIP post-treated at 1750 °C for 3 h with the addition of (a) 0.4 wt %, (b) 0.6 wt.%, (c) 0.8 wt.%, (d) 1.0 wt.% TEOS.

sizes before and after HIP for ceramics were calculated. Figure 6 shows the average grain sizes before and after HIP post-treatment for 5 at.% Sm:LuAG transparent ceramics with 0.4–1.0 wt.% TEOS and 0.05 wt.% CaO. The average grain sizes of ceramics with different amounts of TEOS addition before HIP post-treatment are about 11.5 μm, with little variation. The average grain sizes of ceramics are approximately 15 μm after HIP post-treatment. After HIP post-treatment, there is no significant increase in the average grain sizes of Sm:LuAG ceramics. This is because the HIP post-treatment temperature is close to the vacuum sintering temperature, which does not promote a fast grain growth rate.

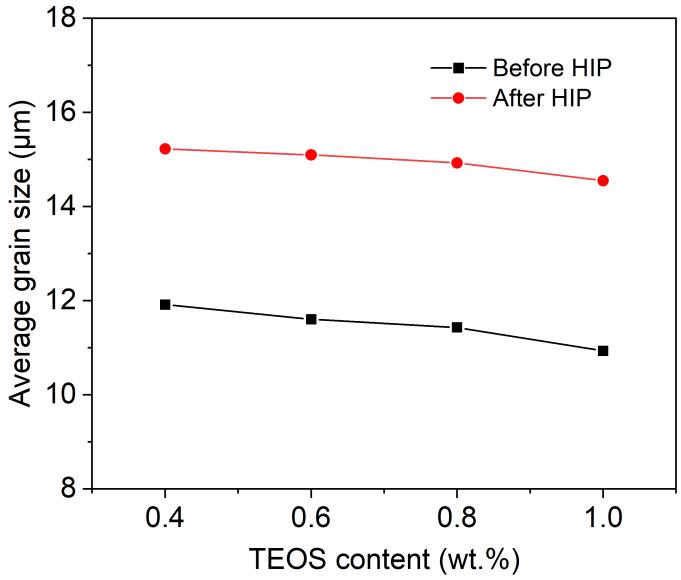

Figure 6. Average grain sizes before and after HIP post-treatment for 5 at.% Sm:LuAG transparent ceramics with 0.4–1.0 wt.% TEOS.

The uniformity of element distribution is one of the key factors affecting the optical quality of transparent ceramics. Inhomogeneous element distribution will lead to light refraction in different aeras of transparent ceramics, which will reduce the optical quality. Therefore, EDS analysis on ceramics sintered at 1825 °C for 5 h and HIP post-treated at 1750 °C for 3 h was performed to study the microscale element homogeneity of Sm:LuAG ceramics. The SEM images and elemental distribution images of ceramics synthesized at 1825 °C are shown in Figure 7. It reveals the distribution of Lu, Al, O and Sm elements in the Sm:LuAG ceramics, the distribution of constituent

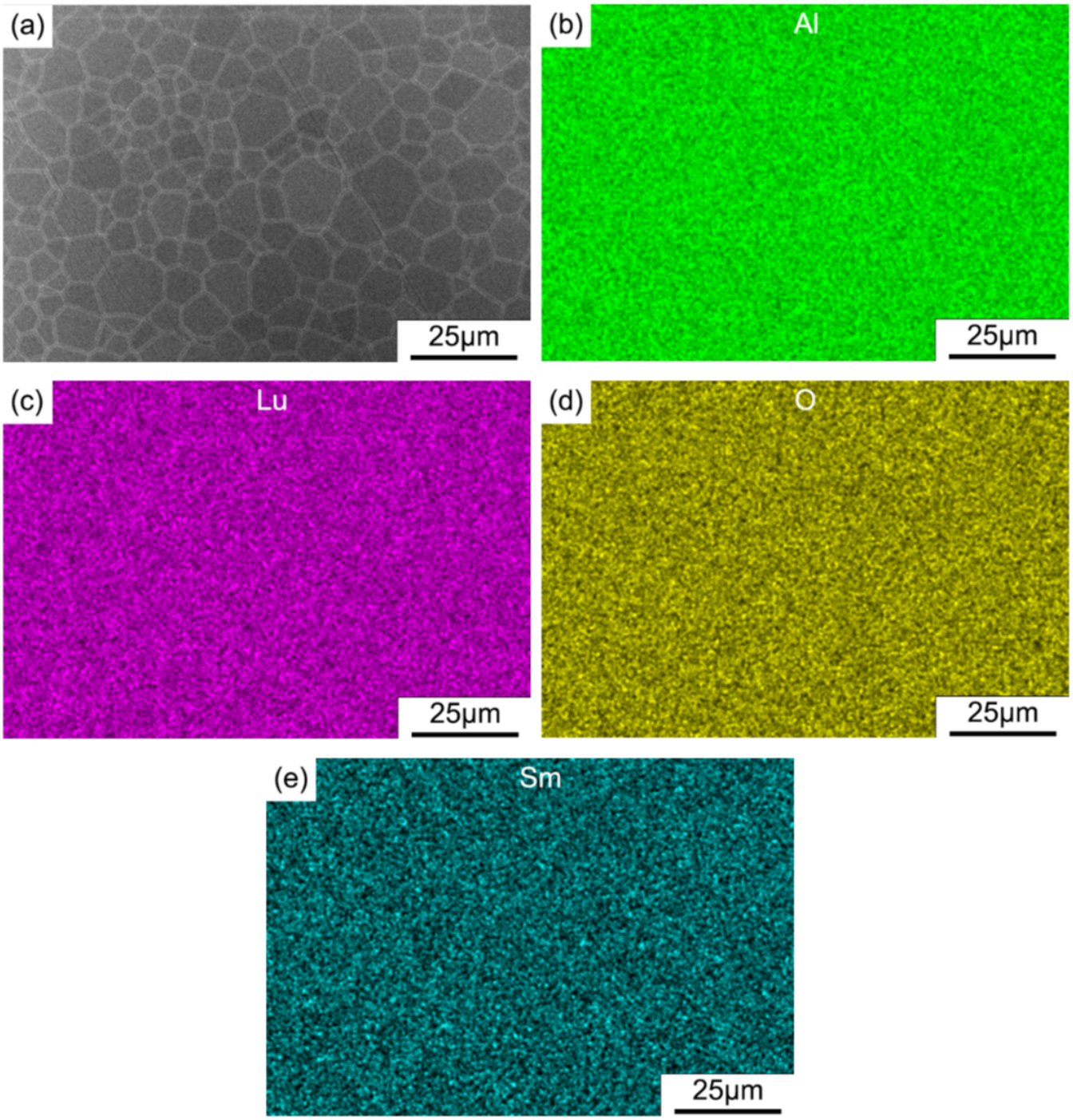

Figure 7. (a) FESEM micrographs of Sm:LuAG ceramics added with 0.8 wt.% TEOS after HIP post-treatment and EDS mapping analysis of Sm:LuAG ceramics: (b) Al, (c) Lu, (d) O and (e) Sm element.

elements and Sm^{3+} ions is uniform both within the grain and along the grain boundaries.

Figure 8 shows the photograph and the in-line transmittance of the 5 at.% Sm:LuAG ceramics with 0.4–1.0 wt.% TEOS and CaO pre-sintered at 1825 °C for 5 h and HIP post-treated at 1750 °C for 3 h. All the ceramic samples were double polished to 1.5 mm thickness. After HIP post-treatment, all the Sm:LuAG ceramics are transparent, and the words below the ceramics can be observed clearly. With the increase of TEOS content from 0.4 wt.% to 1.0 wt.%, the in-line transmittance of Sm:LuAG ceramics first increases and then decreases. According to the LuAG-SiO_2 phase diagram, TEOS begins to form a liquid phase at around 1400 °C, which increases the mass diffusion during sintering and promotes the densification process of ceramics [45]. When the TEOS content is 0.4 wt.% and 0.6 wt.%, less SiO_2 liquid phase is formed, leading

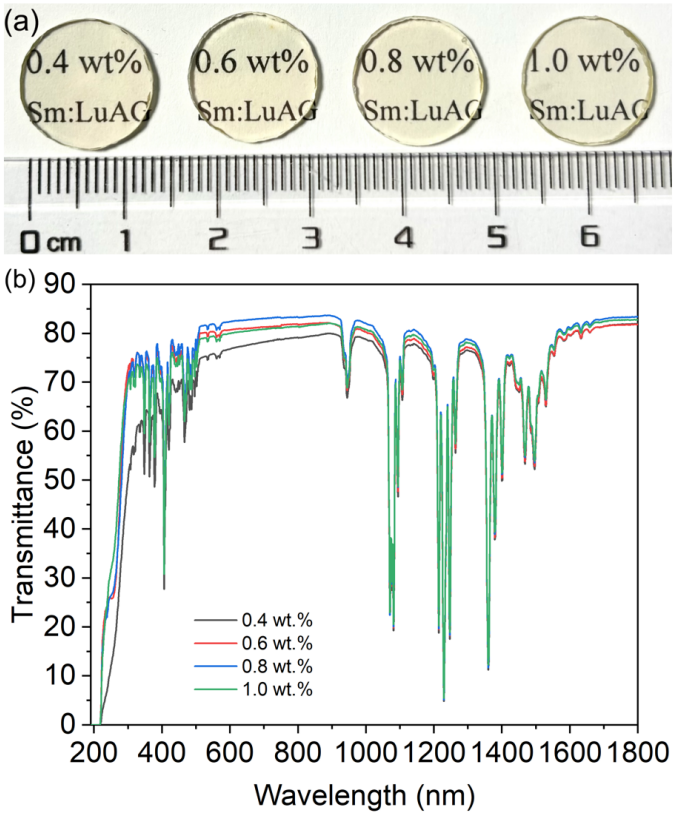

Figure 8. (a) Photograph and (b) the in-line transmittance of the 5 at.% Sm:LuAG ceramics with 0.4–1.0 wt.% TEOS.

to a slower mass diffusion rate. Therefore, there are some residual pores that have not been eliminated in the Sm:LuAG ceramics with 0.4 wt.% and 0.6 wt.% TEOS, as can be seen from Figures 5 and 9. When the TEOS content is 0.8 wt.%, the in-line transmittance of the Sm:LuAG transparent ceramics at 808 nm reaches 83.3%, due to the suitable SiO_2 liquid phase, which promotes the mass diffusion rate and the removal of pores. When the TEOS content is 1.0 wt.%, the optical quality deteriorates due to the increased SiO_2 liquid phase, which makes the mass diffusion rate faster than the pore migration rate, preventing the internal pores from being completely expelled. Therefore, the in-line transmittance of the Sm:LuAG transparent ceramics with 1.0 wt.% TEOS at 808nm is only 81.3%.

Additionally, the high in-line transmittance at the absorption band of Nd:LuAG indicates that using the 5.0 at.% Sm:LuAG ceramics as cladding materials is suitable for edge-pumped lasers.

To study the difference in in-line transmittance and pore distribution of the Sm:LuAG ceramics with different TEOS doping content. Figure 9 shows the optical microscopic images of the 5 at.% Sm:LuAG ceramics with 0.4–1.0 wt.% TEOS and CaO pre-sintered at 1825 °C for 5 h and HIP post-treated at 1750 °C for 3 h. All the Sm:LuAG ceramics have relatively low porosity. With the increase of TEOS doping content from 0.4 wt.% to 1.0 wt.%, the number of pores initially decreases and then increases, which is consistent with the change of in-line transmittance. It is hard to find residual pores in the Sm:LuAG ceramics with 0.8 wt.% TEOS content, which have the highest in-line transmittance of 83.3% at the wavelength of 808 nm.

According to the in-line transmittance of the Sm:LuAG ceramics, the ceramics have high optical quality at the pump wavelength. At the same time, the absorption coefficient of Sm:LuAG ceramics in the laser emission wavelength is also important, which is conducive to suppressing the POs due to ASE from the residual luminescence of Nd^{3+} ions. Figure 10 shows the absorption curves of the 5 at.% Sm:LuAG ceramics with 0.4–1.0 wt.% TEOS and CaO pre-sintered at 1825 °C for 5 h and HIP post-treated at 1750 °C for 3 h. The strong absorption peaks in near-infrared region are located at about 1070 nm, 1229 nm, 1360 nm and 1467 nm. The absorption peak at 1070 nm corresponds to the $^4H_{5/2} \rightarrow ^4 H_{9/2}$ transition of Sm^{3+} ions. With TEOS content increasing from 0.4 to 1.0 wt.%, the absorption coefficients of the ceramics at 1064 nm are 3.49, 3.45, 3.46 and 3.47 cm^{-1}, respectively, showing little variation. The high absorption coefficient at 1064 nm indicate the Sm:LuAG ceramics are promising as cladding materials for Nd:LuAG laser ceramics. According to the requirements of the laser system, the remaining reflection from the cladding material should be:

$$R = \frac{(n_1 - n_2)^2}{(n_1 + n_2)^2} \quad (1)$$

where n_1 is the refractive index of LuAG at 1064 nm, n_2 is the refractive index of air. Then the reflectivity of LuAG is calculated to be 8.5%. After twice absorption of incident emission by Sm:LuAG ceramics, the intensity of the reflected emission is:

$$T = Re^{-2\alpha l} \quad (2)$$

where α is the absorption coefficient of the Sm:LuAG ceramics at 1064 nm, l is the length of the cladding layer along the radial direction. Therefore, when the remaining reflection is $< 0.2\%$, the length of the cladding layer should be > 5.4 mm. With the help of ceramic technology developed in this research, it is possible to prepare high optical quality Sm:LuAG ceramics with 5.4 mm thickness. The Sm-doping concentration of 5.0 at.% is appropriate

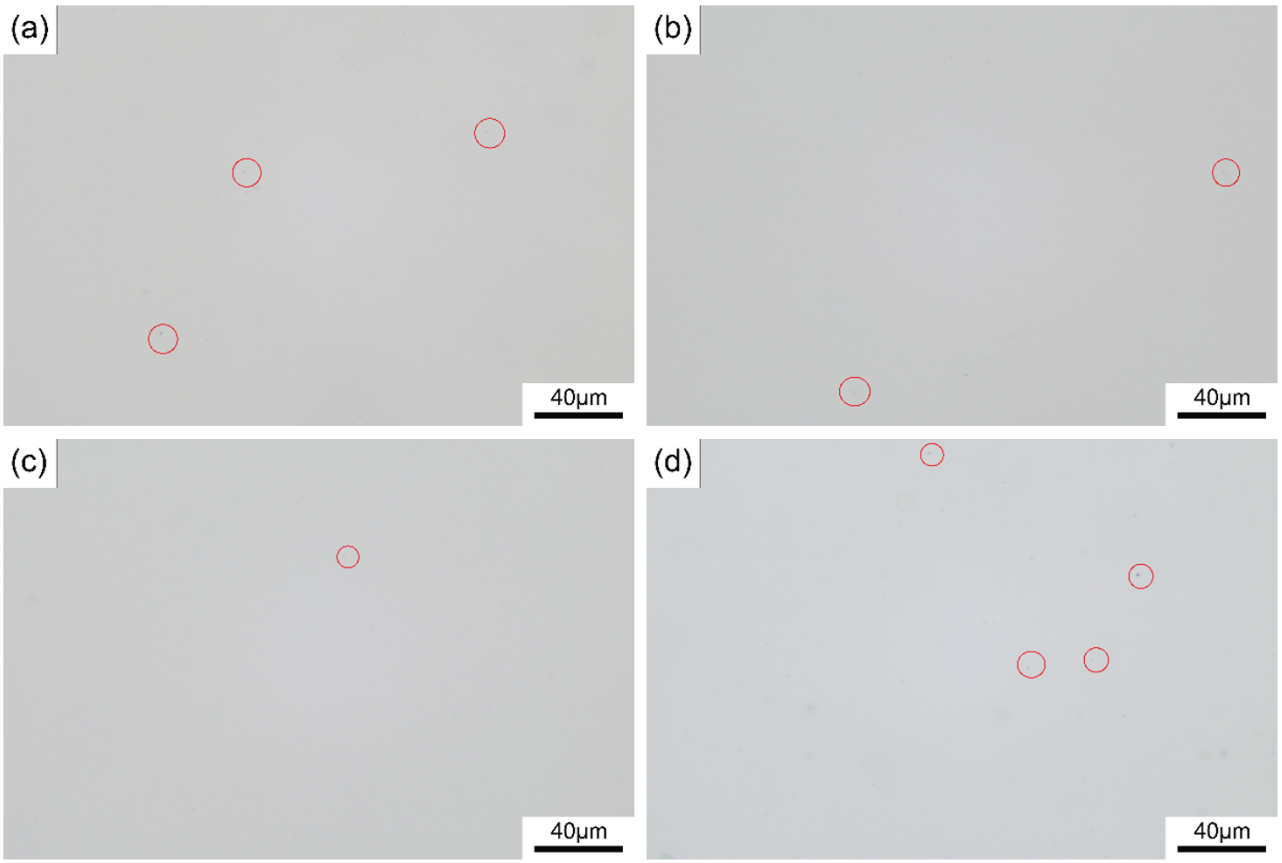

Figure 9. Optical microscopic images of the Sm:LuAG transparent ceramics added with (a) 0.4 wt.%, (b) 0.6 wt.%, (c) 0.8 wt.%, (d) 1.0 wt.% TEOS.

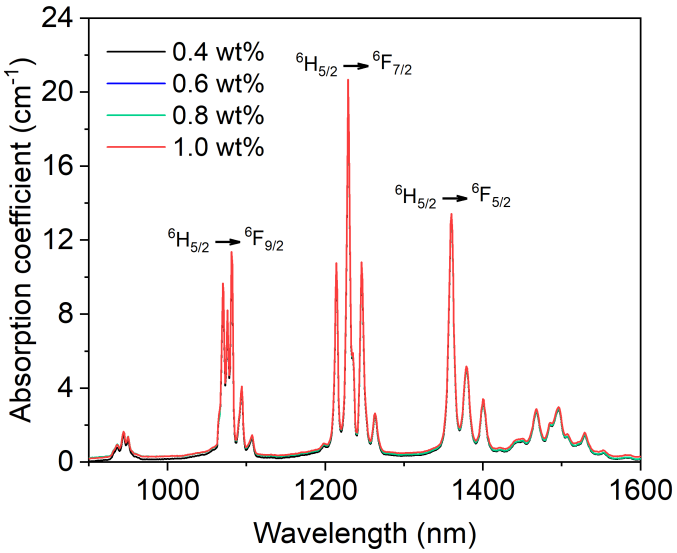

Figure 10. Absorption curves of the 5 at.% Sm:LuAG ceramics added with 0.4–1.0 wt.% TEOS after pre-sintering and HIP post-treatment.

because lower doping concentration brings large-scale ceramics with increased optical loss, and higher doping concentration will cause severe thermal effects.

4 Conclusions

The 5 at.% Sm:LuAG transparent ceramics were fabricated by solid-state reactive sintering, and TEOS and CaO were used as sintering aids. The SiO_2 liquid phase formed during the sintering process increases the mass diffusion rate and promotes the densification process. The Sm:LuAG ceramics with different amounts of TEOS exhibit a dense microstructure after pre-sintering at 1825 °C for 5 h. All ceramic samples show a uniform grain size distribution and the average grain sizes are approximately 15 μm after HIP post-treatment. With the content of TEOS increasing from 0.4 to 1.0 wt.%, the residual pores of Sm:LuAG ceramics decrease and then increase, ceramics with 0.8 wt.% TEOS possess the highest in-line transmittance of 83.3% at 808 nm. The absorption coefficient of the optimal 5 at.% Sm:LuAG ceramics is 3.46 cm^{-1} at 1064 nm, which can effectively suppress the PO and ASE effects. The high in-line transmittance at the pump wavelength of Nd:LuAG and the high absorption coefficient at emission wavelength of Nd:LuAG indicate that the 5 at.% Sm:LuAG ceramics are suitable as cladding materials for edge-pump lasers.

Data Availability Statement

Data will be made available on request.

Funding

This work was supported by the National Key R&D Program of China under Grant 2023YFB3812000.

Conflicts of Interest

The authors declare no conflicts of interest.

Ethical Approval and Consent to Participate

Not applicable.

References

[1] Wan, X., Tan, G., Cai, L., Fu, J., Li, J., & Zhang, Y. (2024). Nd 3+: YAG–Al 2 O 3 nanocrystalline transparent ceramics with high inflexion concentration quenching of Nd 3+ prepared by amorphous crystallization. *Journal of Advanced Ceramics*, *13*(8), 1242-1253.

[2] Qian, Y. A. N. G., ZHENG, Y. T., Shi-Jiang, W. U., Wan-Jun, Y. U., Yang, W. A. N. G., Yong-Dong, Y. U., & Fu-Tian, L. I. U. (2023). A Review on the Preparation of Nanocomposite Oxide Ceramics by Solid State Phase Transformation Method. *Advanced Ceramics*, *44*(5-6), 385-396. [CrossRef]

[3] Sanghera, J., Kim, W., Villalobos, G., Shaw, B., Baker, C., Frantz, J., ... & Aggarwal, I. (2013). Ceramic laser materials: past and present. *Optical Materials*, *35*(4), 693-699. [CrossRef]

[4] Rong, X., Yang, Y., Peng, S., Yang, C., & Wang, D. (2023). Sub-nanosecond diode-pumped passively Q-switched Nd: LuAG ceramic microchip lasers. *Optics & Laser Technology*, *158*, 108901. [CrossRef]

[5] Zhao, C. C., Kim, E. B., Park, Y. J., Logesh, G., Kim, M. J., Lee, J. W., ... & Yoon, S. Y. (2024). Optimization of a TEOS addition on plasma resistance of YAG ceramics. *International Journal of Applied Ceramic Technology*, *21*(5), 3200-3208. [CrossRef]

[6] Han, W. W., Hu, C., Zhou, Z. Z., Ye, J. H., Huang, D., Li, T. S., & Li, J. (2025). Fabrication of Sm:LuAG transparent ceramics with different doping concentrations for cladding from co-precipitated nano-powders. *Journal of Advanced Ceramics*, *14*, 9221129. [CrossRef]

[7] Mang, T. Y. P., Xu, Y., GAO, Q., ZHOU, H., Zhang, Z., Yin, H., ... & SU, L. (2024). Spectroscopic Properties and Optical Clusters in Erbium-doped CaF2, SrF2 and PbF2 Crystals. *Journal of Inorganic Materials*, *39*(3). [CrossRef]

[8] Li, W., Huang, H., Mei, B., Wang, C., Liu, J., Wang, S., ... & Su, L. (2020). Fabrication, microstructure and laser performance of Yb3+ doped CaF2-YF3 transparent ceramics. Ceramics International, 46(11), 19530-19536. [CrossRef]

[9] Kränkel, C. (2014). Rare-earth-doped sesquioxides for diode-pumped high-power lasers in the 1-, 2-, and 3-μm spectral range. *IEEE Journal of Selected Topics in Quantum Electronics*, *21*(1), 250-262. [CrossRef]

[10] Ye, J., Zhou, Z., Hu, C., Wang, Y., Jing, Y., Li, T., ... & Li, J. (2025). Yb: Sc2O3 Transparent Ceramics Fabricated from Co-precipitated Nano-powders: Microstructure and Optical Property. *Wuji Cailiao Xuebao/Journal of Inorganic Materials*, *40*(2), 215-224. [CrossRef]

[11] Li, Q., Liang, F., Wang, J., Xue, Y. L., Ma, J., Liu, P., ... & Tang, D. (2025). Regulation of the sintering trajectory of Ho, Pr: Y 2 O 3 ceramics for 2.9 μm mid-infrared lasers by atmospheric sintering. *Journal of Advanced Ceramics*, *14*(1). [CrossRef]

[12] Yan, L., Xianpeng, Q., Lin, G., Guohong, Z., Tianjin, Z., Shiwei, W., & Hetuo, C. (2024). Preparation of sub-micron spherical Y 2 O 3 particles and transparent ceramics. *Journal of Inorganic Materials*, *39*(6), 691-696. [CrossRef]

[13] Liu, T., Feng, T., Sui, Z., Liu, Q., Gong, M., Zhang, L., ... & Fu, X. (2019). 50 mm-aperture Nd: LuAG ceramic nanosecond laser amplifier producing 10 J at 10 Hz. *Optics Express*, *27*(11), 15595-15603. [CrossRef]

[14] Liu, Q., Gong, M., Liu, T., Sui, Z., & Fu, X. (2016). Efficient sub-joule energy extraction from a diode-pumped Nd: LuAG amplifier seeded by a Nd: YAG laser. *Optics Letters*, *41*(22), 5322-5325. [CrossRef]

[15] Xu, X. D., Wang, X. D., Meng, J. Q., Cheng, Y., Li, D. Z., Cheng, S. S., ... & Xu, J. (2009). Crystal growth, spectral and laser properties of Nd: LuAG single crystal. *Laser Physics Letters*, *6*(9), 678. [CrossRef]

[16] Kaminskii, A. A., Butaeva, T. I., Fedorov, V. A., Bagdasarov, K. S., & Petrosyan, A. G. (1977). Absorption, luminescence, and stimulated emission investigations in Lu3Al5O12-Er3+ Crystals. *physica status solidi (a)*, *39*(2), 541-548. [CrossRef]

[17] Beil, K., Fredrich-Thornton, S. T., Tellkamp, F., Peters, R., Kränkel, C., Petermann, K., & Huber, G. (2010). Thermal and laser properties of Yb:LuAG for kW thin disk lasers. *Optics Express*, *18*(20), 20712–20722. [CrossRef]

[18] Basyrova, L., Maksimov, R., Shitov, V., Baranov, M., Mikhaylovsky, V., Khubetsov, A., ... & Loiko, P. (2019). Effect of SiO2 addition on structural and optical properties of Yb: Lu3Al5O12 transparent ceramics based on laser ablated nanopowders. *Journal of Alloys and Compounds*, *806*, 717-725. [CrossRef]

[19] Sugiyama, M., Fujimoto, Y., Yanagida, T., Yokota, Y., Pejchal, J., Furuya, Y., ... & Yoshikawa, A. (2011). Crystal growth and scintillation properties of Nd-doped Lu3Al5O12 single crystals with different Nd concentrations. *Optical Materials*, *33*(6), 905-908. [CrossRef]

[20] Yan, D., Liu, P., Xu, X., Zhang, J., & Tang, D.

(2018). The phase, microstructure evolution and the Nd3+ function in the fabrication process of LuAG transparent ceramics. *Journal of the European Ceramic Society, 38*(11), 4043-4049. [CrossRef]

[21] Mason, P., Divoký, M., Ertel, K., Pilař, J., Butcher, T., Hanuš, M., ... & Collier, J. (2017). Kilowatt average power 100 J-level diode pumped solid state laser. *Optica, 4*(4), 438-439. [CrossRef]

[22] Divoký, M., Pilař, J., Hanuš, M., Navrátil, P., Denk, O., Severová, P., ... & Mocek, T. (2021). 150 J DPSSL operating at 1.5 kW level. *Optics letters, 46*(22), 5771-5773. [CrossRef]

[23] Ogino, J., Tokita, S., Kitajima, S., Yoshida, H., Li, Z., Motokoshi, S., ... & Kawanaka, J. (2021). 10 J operation of a conductive-cooled Yb: YAG active-mirror amplifier and prospects for 100 Hz operation. *Optics Letters, 46*(3), 621-624. [CrossRef]

[24] Lia, T., Hreniakd, D., & Lia, J. (2024). Effect of Y substitution on the microstructure, magneto-optical, and thermal properties of (Tb1-xYx) 3Al5O12 transparent ceramics. [CrossRef]

[25] Yagi, H., Bisson, J. F., Ueda, K. I., & Yanagitani, T. (2006). Y3Al5O12 ceramic absorbers for the suppression of parasitic oscillation in high-power Nd: YAG lasers. *Journal of luminescence, 121*(1), 88-94. [CrossRef]

[26] Li, X., Hu, C., Liu, Q., Hreniak, D., & Li, J. (2024). Fluoride transparent ceramics for solid-state lasers: A review. *Journal of Advanced Ceramics, 13*(12), 1891–1918. [CrossRef]

[27] Zhang, L., Hu, C., Li, X., Zhou, Z., Li, T., Liu, Y., ... & Li, J. (2024). Effect of Sc substitution on the phase composition, microstructure, and properties of (Tb 1- x Sc x) 3 (Al 1- y Sc y) 2 Al 3 O 12 transparent ceramics. *Journal of Advanced Ceramics, 13*(9), 1442-1452. [CrossRef]

[28] Zhu, K., Zhou, H., Qiu, J., Wang, L. G., & Ye, L. (2022). Optical temperature sensing characteristics of Sm3+ doped YAG single crystal fiber based on luminescence emission. *Journal of Alloys and Compounds, 890*, 161844. [CrossRef]

[29] Huß, R., Wilhelm, R., Kolleck, C., Neumann, J., & Kracht, D. (2010). Suppression of parasitic oscillations in a core-doped ceramic Nd: YAG laser by Sm: YAG cladding. Optics Express, 18(12), 13094-13101. [CrossRef]

[30] Timoshenko, A. D., Matvienko, O. O., Doroshenko, A. G., Parkhomenko, S. V., Vorona, I. O., Kryzhanovska, O. S., ... & Yavetskiy, R. P. (2023). Highly-doped YAG: Sm3+ transparent ceramics: Effect of Sm3+ ions concentration. *Ceramics International, 49*(5), 7524-7533. [CrossRef]

[31] Zhu, Z., Lv, S., Zhang, H., Hui, Y., Lei, H., & Li, Q. (2021). Highly efficient actively Q-switched Nd: YAG laser. *Optics Express, 29*(20), 32325-32332. [CrossRef]

[32] De Vido, M., Ertel, K., Mason, P. D., Banerjee, S., Phillips, P. J., Smith, J. M., ... & Collier, J. L. (2017, February). A 100J-level nanosecond pulsed DPSSL for pumping high-efficiency, high-repetition rate PW-class lasers. In *Solid State Lasers XXVI: Technology and Devices* (Vol. 10082, pp. 124-131). SPIE. [CrossRef]

[33] Lang, Y., Chen, Y., Ge, W., He, J., Zhang, H., Liao, L., ... & Fan, Z. (2018). Actively Q-switched laser with novel Nd: YAG/YAG polygonal active-mirror. *Laser Physics, 28*(3), 035001. [CrossRef]

[34] Ji, S., Huang, W., Feng, T., Pan, L., Wang, J., Lu, X., ... & Li, X. (2021, March). Modeling and measurement of thermal effect in a flashlamp-pumped direct-liquid-cooled split-disk Nd: LuAG ceramic laser amplifier. In *Photonics* (Vol. 8, No. 4, p. 97). MDPI. [CrossRef]

[35] Yagi, H., & Yanagitani, T. (2011). Recent progress in transparent polycrystalline ceramics for optical applications. *The Review of Laser Engineering, 39*(4), 300–305. [CrossRef]

[36] Gonçalvès-Novo, T., Albach, D., Vincent, B., Arzakantsyan, M., & Chanteloup, J. C. (2013). 14 J/2 Hz Yb3+: YAG diode pumped solid state laser chain. *Optics Express, 21*(1), 855-866. [CrossRef]

[37] Ma, J., Lu, T., Zhu, X., Jiang, B., Zhang, P., & Chen, W. (2017). 1.57 MW peak power pulses generated by a diode-pumped Q-switched Nd: LuAG ceramic laser. *Chinese Optics Letters, 15*(12), 121402. [CrossRef]

[38] Kong, W., Tsunekane, M., & Taira, T. (2015). Diode edge-pumped passively Q-switched microchip laser. *Optical Engineering, 54*(9), 090501-090501. [CrossRef]

[39] Li, X., Liu, Q., Guo, L., Hu, C., Wu, J., Toci, G., ... & Li, J. (2025). Effect of powder calcination temperature on the microstructure and laser performance of Yb: CaF2 transparent ceramics. *International Journal of Applied Ceramic Technology, 22*(4), e15108. [CrossRef]

[40] Kijko, V. S., Maksimov, R. N., Shitov, V. A., Demakov, S. L., & Yurovskikh, A. S. (2015). Sintering of transparent Yb-doped Lu2O3 ceramics using nanopowder produced by laser ablation method. *Journal of Alloys and Compounds, 643*, 207-211. [CrossRef]

[41] Vorona, I. O., Yavetskiy, R. P., Parkhomenko, S. V., Doroshenko, A. G., Kryzhanovska, O. S., Safronova, N. A., ... & Baumer, V. N. (2022). Effect of complex Si4++ Mg2+ additive on sintering and properties of undoped YAG ceramics. *Journal of the European Ceramic Society, 42*(13), 6104-6109. [CrossRef]

[42] Jing, Y., Tian, F., Guo, L., Li, T., Wu, J., Ivanov, M., ... & Li, J. (2024). Effect of TEOS content on microstructure evolution and optical properties of Sm: YAG transparent ceramics. *Optical Materials, 147*, 114681. [CrossRef]

[43] HU, C., LIU, Z. Y., LUO, W., CHENG, Z. Q., WANG, Y. B., LI, T. S., & LI, J. (2025). Test Methods for Optical and Opto-Functional Transparent Ceramics. *Advanced Ceramics, 46*(3-4), 286-326. [CrossRef]

[44] Kim, E. B., Zhao, C. C., Park, Y. J., Kim, M. J., Ma, H. J., Kim, H. N., ... & Lee, J. W. (2024). Effect of porosity on etching rate and crater-like microstructure of sintered Al2O3, Y2O3, and YAG ceramics in plasma etching. *Ceramics International*, *50*(9), 15182-15194. [CrossRef]

[45] Stevenson, A. J., Li, X., Martinez, M. A., Anderson, J. M., Suchy, D. L., Kupp, E. R., ... & Messing, G. L. (2011). Effect of SiO2 on densification and microstructure development in Nd: YAG transparent ceramics. Journal of the American Ceramic Society, 94(5), 1380-1387. [CrossRef]

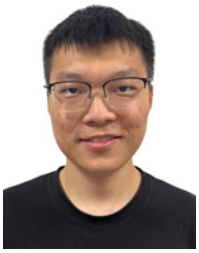

Junhao Ye is currently a Ph.D. candidate at the Shanghai Institute of Ceramics, Chinese Academy of Sciences. He received his Bachelor of Science degree from the College of Physics, Sichuan University in 2022. His doctoral research focuses on the controllable fabrication and properties of sesquioxide transparent ceramics for solid-state lasers gain medium and magneto-optic isolator. (Email: yejunhao22@mails.ucas.ac.cn)

Weiwei Han received his master degree from the School of Microelectronics, Shanghai University in 2025. His master research focuses on the controllable fabrication and properties of Sm:LuAG/Nd:LuAG cladding transparent ceramics for high-power solid-state lasers system. (Email: hw18800205253@163.com)

Zhenzhen Zhou, Ph.D., is an Associate Researcher and Master's Supervisor of the Shanghai Institute of Ceramics, Chinese Academy of Sciences. Her current research primarily focuses on optical functional ceramics, including ceramic phosphors and ceramic scintillators. (Email: zhouzhenzhen@mail.sic.ac.cn)

Chen Hu, Ph.D., is an Associate Researcher and Master's Supervisor of Shanghai Institute of Ceramics, Chinese Academy of Sciences. Mainly engaged in the scintillation performance of BaF_2, Ce:GYGAG ceramic scintillators. (Email: huchen@mail.sic.ac.cn)

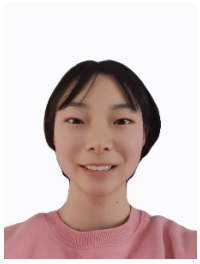

Yiyang Liu is experimentalist in Shanghai Institute of Ceramics, Chinese Academy of Sciences. Mainly engaged in fabrication of high optical quality transparent ceramics. (Email: liuyiyang@mail.sic.ac.cn)

Lexiang Wu is experimentalist in Shanghai Institute of Ceramics, Chinese Academy of Sciences. Mainly engaged in fabrication of high optical quality transparent ceramics. (Email: wulexiang@mail.sic.ac.cn)

Dong Huang received his master degree from the college of Materials Science and Engineering, Jiangsu University. Now, he is an assistant engineer of Shanghai Institute of Ceramics, Chinese Academy of Sciences. His research focuses on the fabrication and scintillation performance of Gd_2O_2S ceramics for X-ray detection imaging and neutron detection imaging. (Email: huangdong@mail.sic.ac.cn)

Tingsong Li is currently a Ph.D. candidate at the Shanghai Institute of Ceramics, Chinese Academy of Sciences. Mainly engaged in basic and applied research on optical and light functional transparent ceramics (including laser ceramics, scintillation ceramics, long afterglow luminescent ceramics, etc.). Current interests are particularly concerned laser ceramics. (Email: litingsong@mail.sic.ac.cn)

Dr. Jiang Li is a professor of Shanghai Institute of Ceramics, Chinese Academy of Sciences (SICCAS). Now he is the deputy director of the transparent ceramics research centre in SICCAS, the associate editors of the Journal of Advanced Ceramics, Journal of Inorganic Materials, and Journal of the American Ceramic Society. Prof. Li's research focuses on laser ceramics, scintillation ceramics, magneto-optical ceramics, ceramic phosphors, and other optical transparent ceramics. He has been selected for four consecutive years as the global top 2% scientists "Lifetime Scientific Impact Rankings" list (2024 edition) released by Stanford University. He was invited to give invited reports in the academic conferences for more than 80 times. He is the coordinator in more than 25 domestic and 8 international collaborative projects so far in the field of transparent and opto-functional ceramics. He produced 484 original papers (9456 Citations, 46 H-index) in refereed journals, 3 co-authored textbooks and 2 co-authored book chapters. (Email: lijiang@mail.sic.ac.cn)